IOPscience iopscience.iop.org

Home Search Collections Journals About Contact us My IOPscience

Finite top mass effects for hadronic Higgs production at next-to-next-to-leading order

This article has been downloaded from IOPscience. Please scroll down to see the full text article.

JHEP11(2009)088

(http://iopscience.iop.org/1126-6708/2009/11/088)

The Table of Contents and more related content is available

Download details:
IP Address: 80.92.225.132
The article was downloaded on 01/04/2010 at 13:31

Please note that terms and conditions apply.

Published by IOP Publishing for SISSA

Received: *September 21, 2009*
Accepted: *November 2, 2009*
Published: *November 19, 2009*

JHEP11(2009)088

Finite top mass effects for hadronic Higgs production at next-to-next-to-leading order

Robert V. Harlander and Kemal J. Ozeren

Fachbereich C, Bergische Universität Wuppertal
42097 Wuppertal, Germany
E-mail: robert.harlander@uni-wuppertal.de,
ozeren@physik.uni-wuppertal.de

Abstract: The first four terms of an expansion in $M_{\rm H}^2/M_t^2$ of the total inclusive cross section for Higgs production in gluon fusion are evaluated through next-to-next-to-leading order QCD. A reliable and precise approximation of the full top mass dependence at NNLO is derived and compared to the frequently used heavy-top limit. It is found that both results agree numerically to better than 0.5% in the Higgs mass range of 100–300 GeV. This validates the higher order results for the inclusive Higgs cross section and justifies the heavy-top limit as a powerful tool for Higgs phenomenology at the LHC and the Tevatron.

Keywords: Higgs Physics, Standard Model

ArXiv ePrint: 0909.3420

© SISSA 2009

doi:10.1088/1126-6708/2009/11/088

Contents

JHEP11(2009)088

1 Introduction

It is expected that the Large Hadron Collider (LHC) will provide insight into the mechanism of electro-weak symmetry breaking. Many of the theoretical models, including the Standard Model (SM), implement it by introducing an as of yet unobserved elementary scalar particle, a so-called Higgs boson. One of the tasks of the LHC is therefore to search for a Higgs boson and to measure its properties (for reviews, see refs. [1–3]).

Precise measurements will require a thorough understanding of the Higgs production cross section. In this respect, the gluon fusion process poses a number of problems: the gluon parton densities need to be known very precisely; the cross section is of order α_s^2 and thus very sensitive to the precise value of this quantity; the radiative corrections and thus the estimated uncertainty from higher order effects is unusually large.

The latter aspect is particularly problematic because the gluon fusion process is loop induced, so that the next-to-leading order (NLO) effects already require a two-loop calculation. Fortunately, it was found that the NLO K-factor is extremely well reproduced in an effective theory approach, obtained by integrating out the top quark from the theory. Details will be discussed below.

Based on this observation, it is commonly assumed that the NNLO corrections, obtained within this effective theory approach, are practically equivalent to the full calculation, at least below the top quark threshold. In fact, almost all radiative corrections beyond NLO have been treated in this framework up to now.

In this paper, we study the quality of this approximation by evaluating subleading terms in the expansion in $1/M_t$. After introducing our notation and the basic formulas in

section 2, we describe our calculational methods in section 3, while the analytic results for the $1/M_t$ expansion are presented in section 4. A matching of the low- to the high energy region is described in section 5 and the numerical analysis is presented in section 6. The conclusions of our findings are drawn in section 7.

2 Higgs production through gluon fusion

The inclusive hadronic cross section for SM Higgs production in proton–(anti-)proton collisions is obtained by convoluting the partonic cross section $\hat{\sigma}_{\alpha\beta\to H+X}$ for the scattering of parton α with parton β by the corresponding parton density functions $\phi_{\alpha/p}(x)$ (PDFs):

$$\begin{aligned}\sigma_{pp'\to H+X}(s) &= \sum_{\alpha,\beta\in\{q,\bar{q},g\}} \int_{M_{\mathrm{H}}^2/s}^1 \mathrm{d}\tau\, \mathcal{E}_{\alpha\beta}(\tau)\, \hat{\sigma}_{\alpha\beta\to H+X}(\hat{s}=\tau s)\,, \\ \mathcal{E}_{\alpha\beta}(\tau) &\equiv \int_\tau^1 \frac{\mathrm{d}x}{x}\left[\phi_{\alpha/p}(x)\phi_{\beta/p'}(\tau/x)\right]\,, \qquad p'\in\{p,\bar{p}\}\,.\end{aligned} \tag{2.1}$$

(In the following, we will shorten or drop the subscripts on $\mathcal{E}$, ϕ, σ, and $\hat{\sigma}$ whenever there is no chance of confusion). In this formula, we have suppressed the dependence on the factorization scale μ_{F} for ϕ and $\hat{\sigma}$, as well as the dependence of σ and $\hat{\sigma}$ on M_t and M_{H}. The partonic cross section $\hat{\sigma}$ is evaluated in terms of a perturbation series in α_s. Its leading order contribution arises from the triangle diagram shown in figure 1(a) (plus the one with opposite fermion direction), where the fermion line can in principle be any of the six quarks. However, due to the Yukawa couplings, the by far dominant contribution is due to top quarks, while the bottom quark has an effect of rougly 7% at the LHC,[1] and 9% at the Tevatron. All lighter quarks can safely be neglected.

NLO QCD corrections to the inclusive cross section have been known for a long time. They were first evaluated for the top quark induced terms in the so-called "heavy-top limit" which will be described in more detail below, and were found to increase the cross section by roughly 70% at the LHC w.r.t. the leading order prediction [4, 5]. This was confirmed by the general result for arbitrary top and bottom quark mass [6, 7].

The large NLO effects clearly asked for the evaluation of the NNLO corrections which, considering its success at NLO, are generally assumed to be well approximated in the heavy-top limit. They lead to another significant increase of the total cross section [8–10], so that its actual value turns out to be roughly a factor of two above the LO prediction for the LHC, and even up to a factor of three at the Tevatron (for the latest compilations, see refs. [11, 12]). Further studies that go beyond the fixed-order NNLO result have not found significant effects and have thus corroborated the stability of the perturbative series (see, e.g. refs. [13, 14]).

The goal of this paper is to go beyond the heavy-top limit in order to test the quality of this approximation. In principle, our approach would also allow us to derive an improved

[1] By "LHC", we refer to pp collisions at 14 TeV center-of-mass energy, although the initial energy of the LHC will be lower; more detailed phenomenological studies at various energies are deferred to a future publication.

JHEP11(2009)088

prediction of the inclusive cross section. However, it will turn out that the heavy-top limit works so well that it reproduces our improved result to better than 0.5% accuracy.

We write the top quark induced partonic cross section as

$$\hat{\sigma}_{\alpha\beta} = \sigma_0 \, \Delta_{\alpha\beta} \,, \tag{2.2}$$

with

$$\sigma_0 = \frac{\pi\sqrt{2}G_{\rm F}}{256} \left(\frac{\alpha_s}{\pi}\right)^2 \tau^2 \left|1 + (1-\tau)\arcsin^2\frac{1}{\sqrt{\tau}}\right|^2 , \qquad \tau = \frac{4M_t^2}{M_{\rm H}^2} \,. \tag{2.3}$$

Here, $G_{\rm F} \approx 1.16637 \cdot 10^{-5}\,\text{GeV}^{-2}$ is Fermi's constant, and throughout this paper, M_t denotes the on-shell top quark mass, and $\alpha_s \equiv \alpha_s^{(5)}(\mu_{\rm R})$ the strong coupling for five active quark flavours at the renormalization scale $\mu_{\rm R}$. The kinetic terms assume the form

$$\Delta_{\alpha\beta}(x) = \delta_{\alpha g}\delta_{\beta g}\,\delta(1-x) + \frac{\alpha_s}{\pi}\Delta^{(1)}_{\alpha\beta}(x) + \left(\frac{\alpha_s}{\pi}\right)^2 \Delta^{(2)}_{\alpha\beta}(x) + \dots \,, \tag{2.4}$$

where

$$x = M_{\rm H}^2/\hat{s} \,. \tag{2.5}$$

The $\Delta^{(n)}$ still depend on M_t, and logarithmically on the renormalization and factorization scales $\mu_{\rm R}$ and $\mu_{\rm F}$. At NLO, the full M_t dependence is known in numerical form [6] (the virtual terms are known analytically [15–17]). At NNLO, only the heavy-top approximation is known, however [8–10]. It will be discussed in more detail in the next section.

Note that in order to arrive at a consistent NNLO result for the hadronic cross section, one needs to evaluate eq. (2.1) not only with an NNLO expression for $\hat{\sigma}$, but also by taking into account expressions for α_s and the PDFs at the appropriate order. In this paper, we use the central set of MSTW2008 [18] which are the latest available NNLO PDFs. A detailed study of the PDF uncertainties is left for a future publication.

Apart from these pure QCD corrections, also the leading electro-weak effects have been evaluated [19–22], and an estimate of the mixed electro-weak/QCD corrections is available [12] as well.

3 Calculation of the $1/M_t$ terms

It is well known that the gluon-Higgs interaction in the heavy-top limit can be expressed in terms of an effective Lagrangian [23]:

$$\mathcal{L}_{\rm eff} = -\frac{H}{4v}\, C_1\, G^a_{\mu\nu} G^{\mu\nu,a} + \mathcal{L}^{(5)}_{\rm QCD} \,, \tag{3.1}$$

where $v = 246\,\text{GeV}$ and the Wilson coefficient C_1 is meanwhile known through $\mathcal{O}(\alpha_s^5)$ [24–26]. For completeness, we quote it here through $\mathcal{O}(\alpha_s^3)$ [27, 28] which is sufficient at NNLO:

$$C_1 = -\frac{1}{3}\frac{\alpha_s}{\pi}\left\{1 + \frac{11}{4}\frac{\alpha_s}{\pi} + \left(\frac{\alpha_s}{\pi}\right)^2\left[\frac{2777}{288} + \frac{19}{16}\ln\frac{\mu^2}{M_t^2} + n_l\left(-\frac{67}{96} + \frac{1}{3}\ln\frac{\mu^2}{M_t^2}\right)\right]\right\} . \tag{3.2}$$

JHEP11(2009)088

$\mathcal{L}^{(5)}_{\rm QCD}$ is the QCD Lagrangian with $n_l = 5$ massless quark flavours.

Instead of working strictly within this effective theory, however, one usually factors out the full leading order top mass dependence from the Higgs production cross section and writes

$$\sigma_\infty(s) = \sum_{\alpha,\beta} \int_{M_{\rm H}^2/s}^1 {\rm d}\tau\, \mathcal{E}_{\alpha\beta}(\tau)\, \hat\sigma_{\alpha\beta,\infty}(\tau s)\,, \qquad \hat\sigma_{\alpha\beta,\infty} \equiv \sigma_0\, \Delta_{\alpha\beta,\infty}\,, \tag{3.3}$$

where σ_0 is given in eq. (2.3), and $\Delta_{\alpha\beta,\infty}$ is evaluated on the basis of eq. (3.1). It is then clear that $\Delta^{(1)}_\infty$ does not depend on M_t, while $\Delta^{(2)}_\infty$ only has a logarithmic M_t-dependence through $C_1(\alpha_s)$. Note that with this *definition of the heavy-top limit*, where the full M_t-dependence in σ_0 is kept, the LO cross section is identical to the one in the full theory.

It was observed long ago [28] that the total cross section at NLO in QCD is approximated by $\sigma^{\rm NLO}_\infty$ to better than 1% up to values of $M_{\rm H} = 2M_t$; even at $M_{\rm H} = 1\,$TeV, the deviation to the exact result remains below 10% (see, e.g., ref. [29]). This precision is quite remarkable, because at higher orders, gluon fusion is a 3-scale process, depending on M_t, $M_{\rm H}$, and the center-of-mass (c.m.) energy $\sqrt{\hat s}$. While at LO $\hat s$ is fixed to $M^2_{\rm H}$, the real radiation of quarks and gluons starting at NLO allows $\sqrt{\hat s}$ to vary from $M_{\rm H}$ up to the hadronic c.m. energy which may reach 14 TeV at the LHC. Considering more exclusive quantities such as p_T-distributions (see ref. [30] and references therein), or even fully differential approaches as in refs. [31, 32], the number of scales increases further and the heavy-top approximation may no longer be under control. Recent studies in this direction can be found in refs. [33, 34].

For the inclusive cross section – which is the subject of this paper – it is usually argued that the reason for the high quality of the approximation in eq. (3.3) is the dominance of soft gluon radiation in the higher order corrections, but a solid theoretical justification and a quantitative error estimate are still unavailable. One may therefore remain in doubt about the applicability of eq. (3.3) beyond NLO. A way to test it is to evaluate subleading terms in $1/M_t$ to the partonic cross section, similar to what was done at NLO in ref. [35]. The effective Lagrangian of eq. (3.1) could clearly be extended to incorporate such terms by including higher dimensional operators (see, e.g., ref. [36]). However, in general at each order in $1/M_t$ the number of operators grows, and renormalization becomes more and more clumsy, for example.

In this paper, instead of constructing an effective Lagrangian, we directly evaluate the Feynman diagrams obtained from the six-flavour Lagrangian by applying the method of asymptotic expansions (for a review, see ref. [37]). At NNLO, the contributing diagrams are at the 3-loop level for the process $gg \to H$, at the 2-loop level for the single real emission processes $gg \to Hg$, $qg \to Hq$, $q\bar q \to Hg$, and at the 1-loop level for the double real emissions $gg \to Hgg$, $gg \to Hq\bar q$, $qg \to Hqg$, $q\bar q \to Hq\bar q$, $qq \to Hqq$ (identical quark flavours), and $qq' \to Hqq'$ (different quark flavours; it is understood that the charge conjugated processes need to be taken into account as well). Each Feynman diagram considered here contains at least one top quark loop. Examples for the various contributions are shown in figure 1.

In our approach, we assume M_t heavier than any other basic scale in the process. This allows us to express all Feynman integrals as convolutions of massive vacuum integrals with

JHEP11(2009)088

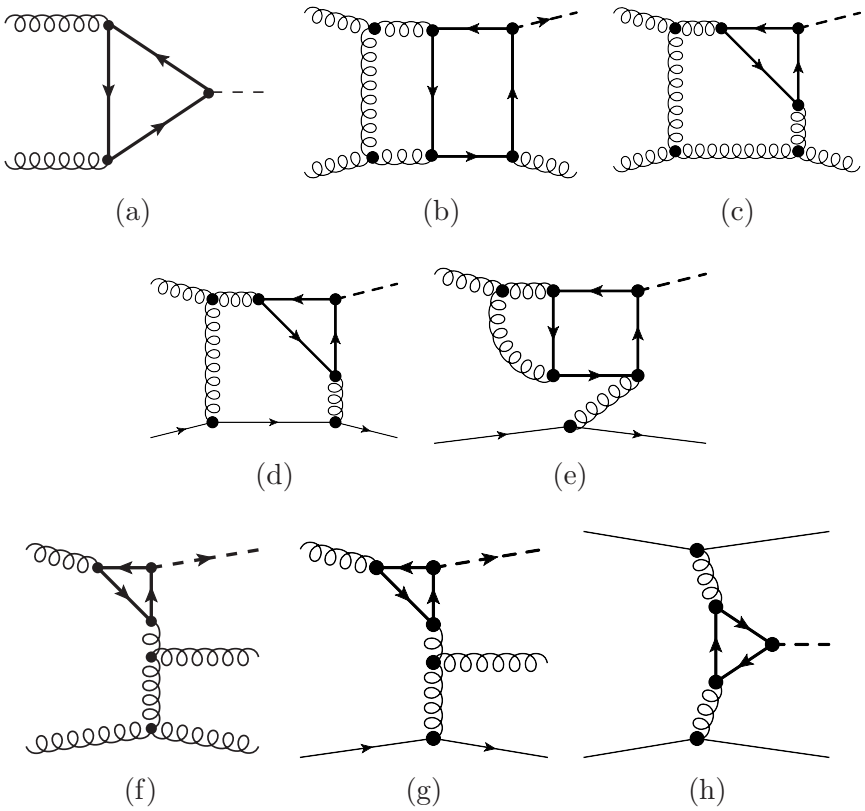

Figure 1. (a) LO Feynman diagram for the gluon fusion process; (b)-(h) Sample Feynman diagrams contributing to the inclusive NNLO cross section for Higgs production in gluon fusion. (b)-(e) single real radiation; (f)-(h) double real radiation.

JHEP11(2009)088

at most three loops, and massless 3/4/5-point functions through 2/1/0 loops, respectively. In fact, the *purely virtual contributions* at NNLO have already been calculated using this method [38, 39],[2] so we will not discuss them in more detail at this point.

For the *double real emission* contributions, the asymptotic expansion is equivalent to the interchange of loop integration and Taylor expansion in p/M_t, where p is any component of the external momenta, and thus one is left only with 1-loop massive tadpole integrals which can be easily evaluated with the help of `MATAD` [40]. The difficulty arises from the phase space integration which we perform in terms of an expansion around $x = 1$ [8] ("soft expansion"). This is fully justified due to the fact that the $1/M_t$-expansion assumes $\sqrt{\hat{s}} < 2M_t$ and thus $x \gtrsim 0.1$ anyway. Apart from that, for the $1/M_t^0$-terms, it was observed that the hadronic cross section converges very well to the full result when successively higher order terms in $(1-x)$ are included in the partonic cross section [8].

The graphical representation of the asymptotic expansion of one of the *single real emission* diagrams is shown in figure 2. The resulting integrals can be calculated by standard means: For the massive tadpoles, we use `MATAD` [40], and the 1-loop tensor integrals are solved using Schwinger parametrisation and integration-by-parts [41]. Both routines

[2]Compared to ref. [38], we have additionally calculated the $1/M_t^6$ term and found agreement with ref. [39].

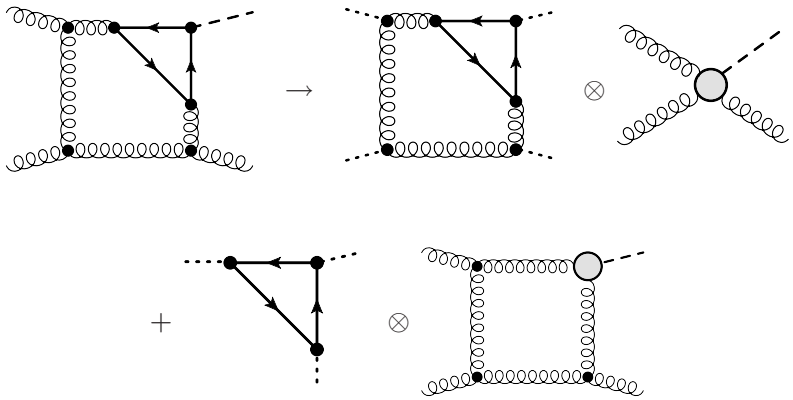

Figure 2. Diagrammatic representation of the asymptotic expansion of a particular Feynman diagram in the limit $\hat{s}, M_{\rm H}^2 \ll 4M_t^2$. The diagrams left of $\otimes$ represent subdiagrams of the original diagram that are to be expanded in the momenta corresponding to the dotted external lines before the loop integration. In this way, it is apparent that the original integral, depending on $\hat{s}$, $M_{\rm H}^2$ and M_t^2, is decomposed into products of "tadpole" integrals with vanishing external momenta and massless four-point functions. The shaded blob in the diagrams right of $\otimes$ represents an effective vertex given by the result of the diagram left of $\otimes$ (for details of asymptotic expansions, see ref.[37], for example).

are embedded in the `q2e/exp` framework [42, 43] which, in combination with the diagram generator `qgraf` [44], provides a fully automatic way to calculate the relevant diagrams, including the procedure of asymptotic expansions. This setup allows for the evaluation of arbitrary orders in the $1/M_t$ expansion, with the only limitation arising from the available computing power. For this publication, we found that the optimal cost/benefit ratio[3] is reached at $\mathcal{O}(1/M_t^6)$, i.e., three orders beyond the heavy-top limit known so far. After multiplication by the corresponding NLO diagrams, we evaluate the phase space integrals in terms of hypergeometric functions depending on $x = M_{\rm H}^2/\hat{s}$ and $\epsilon = (4-D)/2$. Expansion around $\epsilon = 0$ leads to a Laurent series with poles at $\epsilon = 0$ through $\mathcal{O}(1/\epsilon^4)$, and coefficients depending on x through polylogarithms up to the $4^{\rm th}$ degree. Since we calculated the double real emission contributions as expansions in $(1-x)$, we have to expand the single real emission terms in the same way. This is of course trivial from the full x-dependent result. However, also here we can perform the soft expansion before the phase space integration which serves as a useful check.

In the sum of the virtual, single-real, and double-real emission contributions, the $1/\epsilon^4$ poles cancel, and upon UV-renormalization of α_s (for which we adopt the $\overline{\rm MS}$ scheme), M_t and the gluon wave function (both in the on-shell scheme), also the $1/\epsilon^3$-terms drop out. The remaining poles are of infra-red nature, and are absorbed into the PDFs with the help of the usual mass factorization procedure. The relevant convolution integrals are calculated by transforming them into Mellin space (which turns them into simple products) and subsequent inverse Mellin transformation with the help of ref. [45].

[3] As the measure of "benefit" we considered the numerical difference between the highest two terms in the $1/M_t$ expansion.

JHEP11(2009)088

4 Analytical results

A natural decomposition of the kinetic terms to the inclusive cross section is as follows:

$$\Delta^{(n)}_{\alpha\beta} = \delta_{\alpha g}\delta_{\beta g}\left[a^{(n)}\delta(1-x) + \sum_{k=0}^{2n-1} b^{(n)}_k \mathcal{D}_k(x)\right] + h^{(n)}_{\alpha\beta}(x)\,, \tag{4.1}$$

where the $\mathcal{D}_k(x)$ are the usual plus-distributions defined as

$$\int_0^1 \mathrm{d}x\, \mathcal{D}_k(x)\, f(x) \equiv \int_0^1 \mathrm{d}x\, [f(x) - f(1)]\, \frac{\ln^k(1-x)}{1-x} \tag{4.2}$$

for arbitrary functions $f(x)$ (differentiable at $x = 1$). The terms arising from $a^{(n)}$ and $b^{(n)}_k$ are called the "soft+virtual contribution", while $h^{(n)}_{\alpha\beta}$ is referred to as the "hard contribution". The $a^{(n)}$, $b^{(n)}_k$, and $h^{(n)}_{\alpha\beta}(x)$ are functions of the top quark mass. We write them as

$$\{a, b_k, h_{\alpha\beta}(x)\} = \sum_{i\geq 0}\left(\frac{M_\mathrm{H}}{M_t}\right)^i \{a_i, b_{k,i}, h_{\alpha\beta,i}(x)\}\,. \tag{4.3}$$

The leading terms in $1/M_t$, i.e. $i = 0$, have been obtained in refs. [46–48] (soft+virtual) and refs. [8–10] (hard).[4]

Concerning the subleading terms in $1/M_t$, let us begin with the NLO result (terms with odd powers of M_H/M_t vanish):

$$\begin{aligned}
&a^{(1)}_0 = \frac{11}{2} + 6\zeta_2\,, \qquad a^{(1)}_2 = \frac{34}{135}\,, \qquad a^{(1)}_4 = \frac{3553}{113400}\,, \qquad a^{(1)}_6 = \frac{917641}{190512000}\,,\\
&b^{(1)}_{0,i} = 0 \quad \forall\, i \geq 0\,, \qquad b^{(1)}_{1,0} = 12\,, \qquad b^{(1)}_{1,i} = 0 \quad \forall\, i \geq 2\,,
\end{aligned} \tag{4.4}$$

where $\zeta_2 \equiv \pi^2/6$, and we have set $\mu_\mathrm{F} = \mu_\mathrm{R} = M_\mathrm{H}$. For completeness, we have also listed the leading terms in $1/M_t$. Note that the coefficients of the plus distributions are fully determined in the heavy-top limit, i.e., they do not receive $1/M_t$ corrections [6, 35]. $b^{(1)}_{0,0}$ becomes non-zero for $\mu_\mathrm{F} \neq M_\mathrm{H}$ as is obvious from the evolution equations for μ_F.

The hard terms read, for the gg channel:

$$\begin{aligned}
h^{(1)}_{gg,0} &= -\frac{6\,(1-x+x^2)^2}{1-x}\ln x - 12x(2-x+x^2)L(x) - \frac{11}{2}(1-x)^3\,,\\
h^{(1)}_{gg,2} &= -\frac{3x(1-x)}{20}\,, \qquad h^{(1)}_{gg,4} = \frac{(1-x)\left(37+76\,x-83\,x^2+68\,x^3\right)}{11200\,x^2}\,,\\
h^{(1)}_{gg,6} &= \frac{(1-x)\left(3864-4008\,x+4133\,x^2-2668\,x^3+3770\,x^4\right)}{2016000\,x^3}\,,
\end{aligned} \tag{4.5}$$

where

$$L(x) \equiv \ln(1-x)\,. \tag{4.6}$$

[4] In fact, the leading logarithmic hard term was obtained before in ref. [28].

JHEP11(2009)088

For the qg channel (which is identical to the $\bar{q}g$ channel), one finds:

$$\begin{aligned}
h^{(1)}_{qg,0} &= \frac{2}{3}\,(2-2\,x+x^2)\,(2L(x)-\ln x)-1+2\,x-\frac{x^2}{3}\,,\\
h^{(1)}_{qg,2} &= \frac{11(-4+6\,x-3\,x^2+x^3)}{270\,x}\,,\\
h^{(1)}_{qg,4} &= \frac{24409-69264\,x+62052\,x^2-24052\,x^3+6855\,x^4}{1814400\,x^2}\,,\\
h^{(1)}_{qg,6} &= \frac{-181104+690137\,x-1008064\,x^2+658284\,x^3-214280\,x^4+55027\,x^5}{108864000\,x^3}\,.
\end{aligned} \tag{4.7}$$

And finally, for the $q\bar{q}$ channel, it is

$$\begin{aligned}
h^{(1)}_{q\bar{q},0} &= \frac{32}{27}\,(1-x)^3\,, \qquad h^{(1)}_{q\bar{q},2} = \frac{88}{405}\,\frac{(1-x)^3}{x}\,, \qquad h^{(1)}_{q\bar{q},4} = \frac{(1-x)^3\,(3487+842\,x)}{85050\,x^2}\,,\\
h^{(1)}_{q\bar{q},6} &= \frac{(1-x)^3\,(41160+16271\,x+5573\,x^2)}{5103000\,x^3}\,.
\end{aligned} \tag{4.8}$$

Note that except for the $1/M_t^2$ terms for the gg channel which can be found in ref. [35], even this NLO expansion has never been given in the literature. For the sake of brevity, we quote only the first four terms in $1/M_t^2$ here; higher order terms are available from the authors upon request. The same is true for the result for general values of μ_F and μ_R.

There are several observations to be made:

- Pulling out the leading order top mass dependence in terms of σ_0, as done in eq. (2.2), absorbs all the logarithmic x and $(1-x)$ dependence into the leading $1/M_t$ terms.

- In general, each power in M_H^2/M_t^2 is accompanied by a power in $1/x$. This is a consequence of assuming that the top quark mass is the heaviest scale of the process. The expansion therefore is not just in M_H^2/M_t^2 as suggested by the form of eq. (4.3), but also in $\hat{s}/M_t^2$ which leads to

$$\frac{\hat{s}}{M_t^2} = \frac{M_H^2}{M_t^2}\,\frac{1}{x}\,. \tag{4.9}$$

  These terms are a sign of the breakdown of the heavy-top limit: for large $\hat{s}$, they lead to a singular behaviour of the partonic cross section that becomes stronger with every order in $1/M_t^2$. The consequence is that the corresponding hadronic cross section does not converge as successively higher orders in $1/M_t$ an included. Our solution of this problem will be described below.

- For the gg channel, the coefficient of the $1/x$ term at $i = 2$ turns out to vanish. The strategy of ref. [35] for analysing the $1/M_t$ corrections at NLO was therefore to discard the terms with $i > 2$ in the gg channel, and to replace the $1/M_t$ expansion for the other channels by the exact result (which is much easier to obtain than for the gg channel). For the NNLO case, we do not have that option, because the calculation of the full mass dependence is currently out of reach. As mentioned before, we will discuss the problem of low x (large $\hat{s}$) in more detail in section 5.

JHEP11(2009)088

Let us now turn to the NNLO results. For the soft+virtual terms, we obtain:

$$
\begin{aligned}
a_0^{(2)} &= \frac{11399}{144} + \frac{19}{8} l_{Ht} + \frac{133}{2}\zeta_2 - \frac{165}{4}\zeta_3 - \frac{9}{8}\zeta_4 + n_l \left(-\frac{1189}{144} + \frac{2}{3} l_{Ht} - \frac{5}{3}\zeta_2 + \frac{5}{6}\zeta_3 \right) , \\
a_2^{(2)} &= -\frac{47437199}{1244160} + \zeta_2 \left(\frac{89}{45} + \frac{7}{45} \ln 2 \right) + \frac{1909181}{55296}\,\zeta_3 + \frac{883}{1080}\, l_{Ht} \\
&\quad + n_l \left(\frac{14563}{48600} - \frac{281}{2880}\, l_{Ht} - \frac{7}{90}\,\zeta_2 \right) , \\
a_4^{(2)} &= -\frac{998645169149}{117050572800} + \zeta_2 \left(\frac{9677}{37800} + \frac{857}{37800}\, \ln 2 \right) + \frac{267179777}{35389440}\,\zeta_3 + \frac{4039}{51840}\, l_{Ht} \\
&\quad + n_l \left(\frac{4565713}{285768000} - \frac{857}{75600}\,\zeta_2 - \frac{193927}{21772800}\, l_{Ht} \right) , \\
a_6^{(2)} &= -\frac{1712964005499545249}{39328992460800000} + \zeta_2 \left(\frac{646571}{15876000} + \frac{17881}{4536000} \ln 2 \right) + \frac{5756378217151}{158544691200}\,\zeta_3 \\
&\quad + \frac{88077779}{7620480000}\, l_{Ht} + n_l \left(\frac{8432587511}{4800902400000} - \frac{17881}{9072000}\,\zeta_2 - \frac{111726613}{91445760000}\, l_{Ht} \right) ,
\end{aligned}
$$

$$
\begin{aligned}
b_{0,0}^{(2)} &= -\frac{101}{3} + 33\,\zeta_2 + \frac{351}{2}\,\zeta_3 + n_l \left(\frac{14}{9} - 2\,\zeta_2 \right) , \\
b_{1,0}^{(2)} &= 133 - 90\,\zeta_2 - \frac{10}{3}\, n_l , \qquad b_{1,2}^{(2)} = \frac{136}{45} , \qquad b_{1,4}^{(2)} = \frac{3553}{9450} , \qquad b_{1,6}^{(2)} = \frac{917641}{15876000} , \\
b_{2,0}^{(2)} &= -33 + 2\, n_l , \qquad\qquad b_{2,i}^{(2)} = 0 \quad \forall\ i \geq 2 , \\
b_{3,0}^{(2)} &= 72 , \qquad\qquad b_{3,i}^{(2)} = 0 \quad \forall\ i \geq 2 ,
\end{aligned}
\tag{4.10}
$$

where $\zeta_n \equiv \zeta(n)$ is Riemann's zeta function with values

$$
\zeta_2 = \frac{\pi^2}{6} = 1.64493\ldots , \qquad \zeta_3 = 1.20206\ldots , \qquad \zeta_4 = \frac{\pi^4}{90} = 1.08232\ldots , \tag{4.11}
$$

and

$$
l_{Ht} = \ln \frac{M_{\rm H}^2}{M_t^2} . \tag{4.12}
$$

The various hard contributions are evaluated as expansions around $x = 1$. We quote them through $\mathcal{O}(1-x)$ for the sake of brevity. Terms through order $(1-x)^{13}$, for arbitrary values of $\mu_{\rm F}$ and $\mu_{\rm R}$, are available upon request from the authors.

For the gg channel, we find

$$
\begin{aligned}
h_{gg,0}^{(2)} =& \frac{1453}{12} - 147\,\zeta_2 - 351\,\zeta_3 + L(x) \left(-\frac{1193}{4} + 180\,\zeta_2 \right) + \frac{411}{2}\, L^2(x) - 144\, L^3(x) \\
&+ n_l \left(-\frac{77}{18} + 4\,\zeta_2 + \frac{101}{12}\, L(x) - 4\, L^2(x) \right) \\
&+ (1-x) \Bigg[-\frac{3437}{4} + \frac{1017}{2}\,\zeta_2 + \frac{1053}{2}\,\zeta_3 + L(x) \left(\frac{2379}{2} - 270\,\zeta_2 \right) \\
&- \frac{2385}{4}\, L^2(x) + 216\, L^3(x) + n_l \left(\frac{395}{24} - \frac{22}{3}\,\zeta_2 - \frac{45}{2}\, L(x) + \frac{22}{3}\, L^2(x) \right) \Bigg] + \cdots ,
\end{aligned}
$$

JHEP11(2009)088

$$
\begin{aligned}
h^{(2)}_{gg,2} =& \frac{68}{45} - \frac{272}{45}\,L(x) + (1-x)\bigg[- \frac{6661}{1200} - \frac{9}{80}\,\zeta_2 + \frac{172}{15}\,L(x) - \frac{81}{80}\,L^2(x) - \frac{27}{40}\,l_{Ht} \\
&+ n_l\left(\frac{11}{80} - \frac{1}{20}L(x)\right)\bigg] + \cdots\,, \\
h^{(2)}_{gg,4} =& \frac{3553}{18900} - \frac{3553}{4725}\,L(x) + (1-x)\bigg[- \frac{1837333}{10584000} + \frac{21}{3200}\,\zeta_2 + \frac{49927}{50400}\,L(x) \\
&+ \frac{189}{3200}\,L^2(x) + \frac{471}{11200}\,l_{Ht} + n_l\left(- \frac{659}{67200} + \frac{7}{2400}\,L(x)\right)\bigg] + \cdots\,, \\
h^{(2)}_{gg,6} =& \frac{917641}{31752000} - \frac{917641}{7938000}\,L(x) + (1-x)\bigg[\frac{13461173}{635040000} + \frac{1697}{896000}\,\zeta_2 + \frac{5644979}{42336000}\,L(x) \\
&+ \frac{15273}{896000}\,L^2(x) + \frac{15731}{1344000}\,l_{Ht} + n_l\left(- \frac{23347}{8064000} + \frac{1697}{2016000}\,L(x)\right)\bigg] + \cdots\,.
\end{aligned}
\tag{4.13}
$$

Here and in the following equations, the ellipse indicate higher orders in $(1-x)$. The qg (and $\bar{q}g$) channel reads

$$
\begin{aligned}
h^{(2)}_{qg,0} =& \frac{11}{27} + \frac{29}{6}\,\zeta_2 + \frac{311}{18}\,\zeta_3 + \frac{85}{36}\,L^2(x) + \frac{367}{54}\,L^3(x) \\
&+ n_l\left(\frac{13}{81} - \frac{2}{3}\,L(x) + \frac{1}{18}\,L^2(x)\right) + L(x)\left(\frac{341}{18} - \frac{50}{9}\,\zeta_2\right) \\
&+ (1-x)\bigg[- \frac{959}{18} + 8\,\zeta_2 + \frac{433}{9}\,L(x) - \frac{33}{2}\,L^2(x) + \frac{4}{9}\,n_l\,L(x)\bigg] + \cdots\,, \\
h^{(2)}_{qg,2} =& \frac{68}{405} + \frac{136}{405}\,L(x) + (1-x)\bigg[- \frac{62737}{24300} - \frac{539}{1080}\,\zeta_2 + \frac{4367}{3240}\,L(x) - \frac{187}{360}\,L^2(x) \\
&- \frac{1441}{3240}\,l_{Ht} + n_l\left(\frac{44}{405} - \frac{11}{270}\,L(x)\right)\bigg] + \cdots\,, \\
h^{(2)}_{qg,4} =& \frac{3553}{170100} + \frac{3553}{85050}\,L(x) + (1-x)\bigg[- \frac{66227323}{285768000} - \frac{2947}{129600}\,\zeta_2 + \frac{26401}{388800}\,L(x) \\
&- \frac{7157}{302400}\,L^2(x) - \frac{37481}{2721600}\,l_{Ht} + n_l\left(\frac{421}{85050} - \frac{421}{226800}\,L(x)\right)\bigg] + \cdots\,, \\
h^{(2)}_{qg,6} =& \frac{917641}{285768000} + \frac{917641}{142884000}\,L(x) + (1-x)\bigg[- \frac{1018432391}{34292160000} \\
&- \frac{39011}{15552000}\,\zeta_2 + \frac{2460599}{326592000}\,L(x) - \frac{94741}{36288000}\,L^2(x) - \frac{96389}{65318400}\,l_{Ht} \\
&+ n_l\left(\frac{5573}{10206000} - \frac{5573}{27216000}\,L(x)\right)\bigg] + \cdots\,.
\end{aligned}
\tag{4.14}
$$

The remaining channels only start at higher orders in $(1-x)$:

$$
\begin{aligned}
&h^{(2)}_{q\bar{q},0} = h^{(2)}_{qq,0} = h^{(2)}_{qq',0} = (1-x)\bigg[\frac{20}{9} - \frac{16}{9}\,\zeta_2 - \frac{16}{9}\,L(x) + \frac{16}{9}\,L^2(x)\bigg] + \cdots\,, \\
&h^{(2)}_{q\bar{q},i} = h^{(2)}_{qq,i} = h^{(2)}_{qq',i} = \mathcal{O}((1-x)^2) \quad \forall\; i \geq 2\,.
\end{aligned}
\tag{4.15}
$$

Again, we have included the known leading terms in $1/M_t$ for the sake of completeness.

JHEP11(2009)088

5 Small-x behaviour

As pointed out above, the $1/M_t$ expansion cannot give the proper result in the low-x (large-$\hat{s}$) region, which is why the $(1-x)$-expansion in this approach is no worse than the full x dependence. Fortunately, in ref. [49], it was derived that the leading small-x behaviour of the partonic cross section is given by ($\mu_F = \mu_R = M_H$)

$$\hat{\sigma}_{gg}^{(1)}(x) = 3\,\sigma_0\,\mathcal{C}^{(1)} + \mathcal{O}(x)\,, \qquad \hat{\sigma}_{gg}^{(2)}(x) = -9\,\sigma_0\,\mathcal{C}^{(2)}\ln x + c + \mathcal{O}(x)\,, \tag{5.1}$$

where the coefficients $\mathcal{C}^{(1)}$ and $\mathcal{C}^{(2)}$ are available in ref. [49] in the form of a numerical table for various values of M_t/M_H out of which we constructed simple interpolating functions. The constant c was undetermined. Note that eq. (5.1) is the actual limit of $\hat{s} \to \infty$, i.e., it is *not* derived in the heavy-top limit.

We may use this additional information to improve our result in the following way:[5]

$$\begin{aligned}
\hat{\sigma}_{gg}^{(1)}(x) &= \hat{\sigma}_{gg}^{(1),N}(x) + (1-x)^{N+1}\left[3\,\sigma_0\mathcal{C}^{(1)} - \hat{\sigma}_{gg}^{(1),N}(0)\right]\,,\\
\hat{\sigma}_{gg}^{(2)}(x) &= \hat{\sigma}_{gg}^{(2),N}(x) - 9\,\sigma_0\mathcal{C}^{(2)}\left[\ln x + \sum_{k=1}^{N}\frac{1}{k}(1-x)^k\right]\,,
\end{aligned} \tag{5.2}$$

where $\hat{\sigma}_{gg}^{(n),N}$ denotes the expansion of the partonic cross section around $x = 1$ through $\mathcal{O}((1-x)^N)$. Note that $\hat{\sigma}_{gg}^{(1)}(x)$ and $\hat{\sigma}_{gg}^{(2)}(x)$ have the correct behaviour for $x \to 0$ and $x \to 1$ up to the orders considered. In this way, we arrive at smooth functions that approximate the full partonic cross section over the full x-range. In order to illustrate the quality of this method, figure 3 shows $\hat{\sigma}_{gg}^{(1)}(x)$ together with the soft expansion $\hat{\sigma}_{gg}^{(1),N}(x)$ for $N = 8$, as well as $\hat{\sigma}_{gg,\infty}^{(1)}$, i.e., the full x-dependence of the heavy-top result. All expressions include top mass corrections through $\mathcal{O}(1/M_t^6)$; the curves are normalized by σ_0.

In order to be able to directly compare figure 3 with ref. [50] (which updates the numerics of ref. [49]), the scales in figure 3 (a) are chosen identical to those of figures 1 and 2 in ref. [50]. For the same reason, we set $M_t = 170.9\,\text{GeV}$ at this point, in contrast to the actual numerical section of this paper where the current world average for M_t is used. And finally, the curve for $\hat{\sigma}_{gg,\infty}^{(1)}$ in the heavy-top limit is included (i.e., only the $1/M_t^0$ terms), as in ref. [50]. In case one is misled by the apparently large effect, figure 3 (b) shows the same curves on a linear scale. In fact, as will become obvious shortly, the effect of this matching on the *hadronic* cross section is rather small compared to using just the pure soft expansion $\hat{\sigma}_{gg}^{(1),N}(x)$ (cf. figure 5 below).

Similarly, figure 4 shows the NNLO partonic cross section (gluon-gluon channel) as constructed from eq. (5.2), again with choice of scales and set of parameters as in ref. [50]. The agreement to the result obtained in ref. [50] is good, with a small difference on the unknown constant c in eq. (5.2). The effect of the matching on the *hadronic* cross section is completely negligible when compared to the pure soft expansion $\hat{\sigma}_{gg}^{(2),N}(x)$ (cf. figure 7 below). This is of course due to a suppression of the large-x region by the parton densities.

[5] The upper equation essentially corresponds to the matching procedure suggested in ref. [49].

JHEP11(2009)088

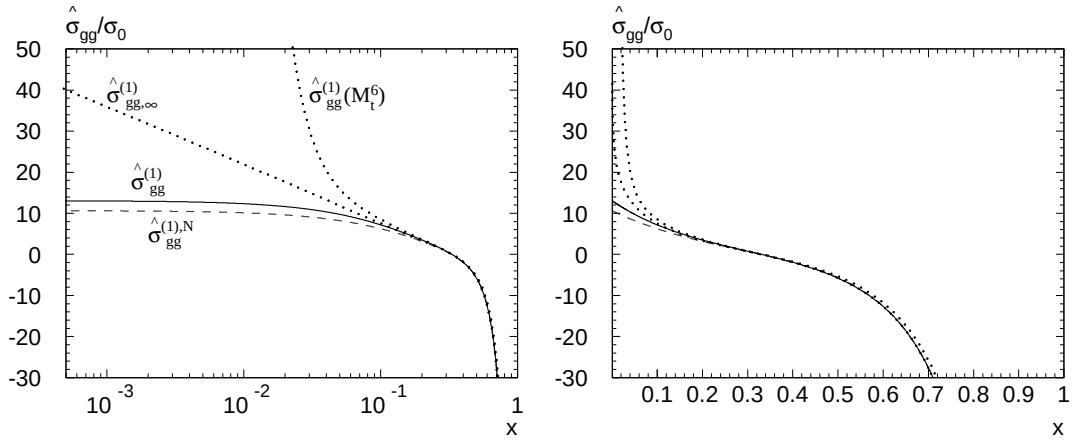

Figure 3. The NLO contribution to the partonic cross section $\hat{\sigma}_{gg}^{(1)}$ as a function of $x = M_{\rm H}^2/\hat{s}$ on a logarithmic (a) and a linear scale (b). The expansion in $(1-x)$ converges up to the threshold $x = M_{\rm H}^2/(4M_t^2) \approx 0.14$. This expansion, through $(1-x)^8$, is displayed as the dashed curve, $\hat{\sigma}_{gg}^{(1),N}$, $N = 8$. The full x-dependence of the $1/M_t$ expansion is shown as the dotted curves (lower: leading term in $M_{\rm H}/M_t$, upper: including terms of order $1/M_t^6$). The solid line is the combination of the $(1-x)$-expansion with the leading behaviour at $x \to 0$, cf. eq. (5.1).

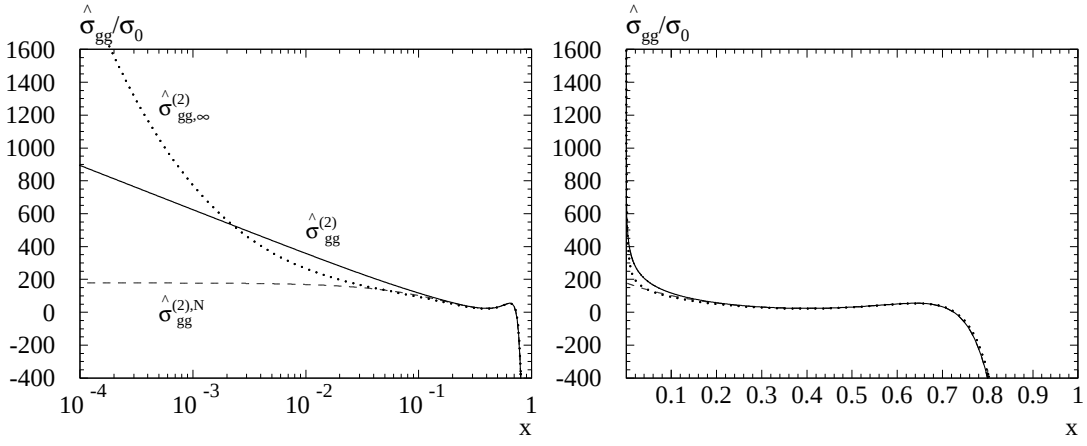

Figure 4. Same as figure 3, but at NNLO. The dotted line is the full x-dependence of the $1/M_t^0$ result.

6 Numerical results

Unless stated otherwise, in all our numerical analyses in this paper, we use $M_t = 173.1\,\text{GeV}$ and set $\mu_{\rm F} = \mu_{\rm R} = M_{\rm H}$. The latter restriction shall be sufficient for this first study of the top mass effects; more detailed phenomenological studies, including scale variations, are left for a future publication.

JHEP11(2009)088

6.1 Next-to-leading order

The natural extension of the heavy top limit of eq. (3.3) would be to use eq. (2.2) with the full top mass dependence in σ_0 and the $1/M_t$ expansion of $\Delta_{\alpha\beta}$ as given in section 4, and to match the result to the large-$\hat{s}$ region as defined in section 5. However, in order to strictly test the heavy-top limit, we prefer to apply a consistent $1/M_t$ expansion to the partonic cross section, without factoring out the LO mass dependence. Once the convergence of this $1/M_t$ expansion and its consistency with the heavy-top limit of eq. (3.3) is shown, one could try to derive an "improved heavy-top limit" by keeping the full mass dependence in σ_0. However, as we will see, the improvement achieved in this way is well below any expected experimental accuracy.

At NLO, we therefore define

$$\hat{\sigma}^{\text{NLO}}_{\alpha\beta}(M_t^n) = \sigma_0\,\delta_{\alpha g}\delta_{\beta g}\delta(1-x) + \frac{\alpha_s}{\pi}\,\hat{\sigma}^{(1)}_{\alpha\beta}(M_t^n)\,, \tag{6.1}$$

where $\hat{\sigma}^{(1)}_{\alpha\beta}(M_t^n)$ is the NLO contribution to the partonic cross section evaluated as an expansion through $\mathcal{O}((M_{\text{H}}/M_t)^n)$. It is obtained by expanding $\sigma_0\Delta^{(1)}_{\alpha\beta}$ with σ_0 and $\Delta^{(1)}_{\alpha\beta}$ from eqs. (2.3), (4.1), (4.4)–(4.8) in terms of $1/M_t$, and applying the matching procedure of eq. (5.2). The corresponding hadronic quantity derived from eq. (6.1) is denoted by $\sigma^{\text{NLO}}_{\alpha\beta}(M_t^n)$, as usual. Note that it also depends on the depth of the expansion in $(1-x)$.

First, we look at the convergence of the $1/M_t$ expansion of the gg channel alone, whose low-x behaviour is implemented as described in section 5. Figure 5 shows the ratio of $\sigma^{\text{NLO}}_{gg}(M_t^n)$, keeping various orders in $1/M_t$, to the fully mass dependent result $\sigma^{\text{HIGLU}}_{gg}$ (dashed: $1/M_t^n$, $n = 0,\ldots,8$; solid: $1/M_t^{10}$). The dotted line corresponds to the pure soft expansion result σ^{N}_{gg}, without matching to the low-x behaviour. The convergence towards the exact result is excellent, both for the LHC (a) and the Tevatron (b). The slightly better behaviour for the Tevatron is due to the smaller high-energy region. The effect of the matching from section 5 is rather small.

Unfortunately, the analytic low-x behaviour is currently not known for the subleading channels (qg, $q\bar{q}$, and also the NNLO channels qq, qq'). However, their numerical contribution at NLO is very small (for "reasonable" values of $\mu_{\text{F}} \sim M_{\text{H}}$): for Higgs masses between 100 and 300 GeV, the qg contribution is at the few percent level ($< 4\%$) and the $q\bar{q}$ at the permille level.

One could therefore just proceed by ignoring the $1/M_t$-corrections at NNLO for all but the gg channel. At NLO, however, we observe that we can nevertheless improve the prediction by including the $1/M_t$ and $(1-x)$ expansion of the subleading terms up to a certain depth beyond which the convergence properties of the series for the individual channels deteriorate, as is typical for an asymptotic series. Applying this criterion at NLO allows us to include the terms through order $1/M_t^{10}$ for the qg channel, but only the first two terms for the $q\bar{q}$ channel. The convergence of the expansion in $(1-x)$ is excellent (see below).

This "optimal" result will be denoted by $\sigma^{\text{NLO}}(M_t)$. It is shown in figure 6, divided by the exact mass dependence, both for a 14 TeV proton-proton collider (a), and for a 1.96 TeV proton–anti-proton collider (b). One observes a nice convergence for the soft expansion towards a result that reproduces the full mass dependence at the sub-percent level. For

JHEP11(2009)088

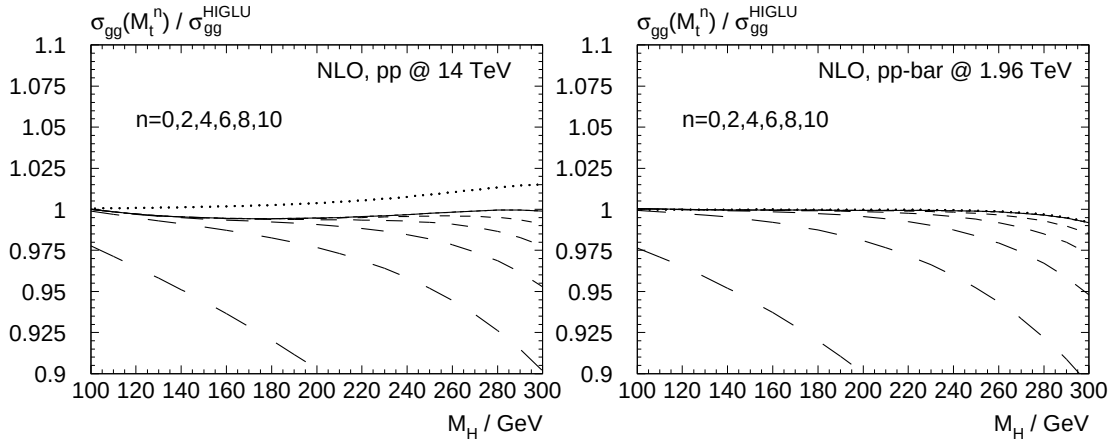

Figure 5. Ratio of the gg induced component of the NLO hadronic cross section as obtained from eq. (5.2) to the value obtained from HIGLU [51], when keeping successively higher orders in $1/M_t$ (decreasing dash-length corresponds to increasing order); the dotted line is the result obtained from the pure soft expansion $\hat{\sigma}_{gg}^{(1),N}$ through order $1/M_t{}^{10}$ without the matching of eq. (5.2).

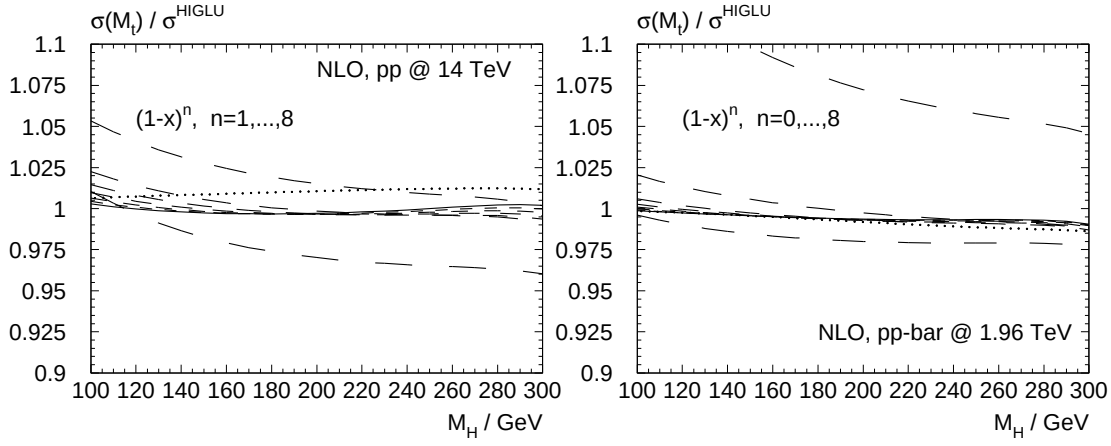

Figure 6. Solid: the final result for the NLO cross section, divided by the full top mass dependent result as obtained from HIGLU [51]. The dashed lines correspond to various orders in the $(1-x)$ expansion and nicely demonstrate the quality of the convergence. The dotted lines represent the result of the heavy-top limit at NLO (eq. (3.3)).

comparison, the figure also contains the ratio of the heavy-top limit to the exact mass dependence (dotted line) which deviates from one at the percent level, as pointed out before.

6.2 Next-to-next-to-leading order

In analogy to eq. (6.1), we define

$$\hat{\sigma}_{\alpha\beta}^{\mathrm{NNLO}}(M_t^n) = \sigma_0 \left[\delta_{\alpha g}\delta_{\beta g}\delta(1-x) + \frac{\alpha_s}{\pi}\,\Delta_{\alpha\beta,\infty}^{(1)}\right] + \left(\frac{\alpha_s}{\pi}\right)^2 \hat{\sigma}_{\alpha\beta}^{(2)}(M_t^n)\,, \tag{6.2}$$

JHEP11(2009)088

where $\hat{\sigma}^{(2)}_{\alpha\beta}(M_t^n)$ is obtained by expanding $\sigma_0\Delta^{(2)}_{\alpha\beta}$, with σ_0 and $\Delta^{(2)}_{\alpha\beta}$ from eqs. (2.3), (4.1), (4.10)–(4.15), in terms of $1/M_t$, up to power n, and applying the matching procedure of eq. (5.2). We already know that the first term in eq. (6.2) is an excellent approximation to the full top mass dependent result, and therefore eq. (6.2) provides a suitable quantity to compare the heavy-top result of eq. (3.3) to the $1/M_t$ expansion.

Again, we first look at the convergence of the $1/M_t$ expansion of the gg channel alone, whose low-x behaviour is implemented as described in section 5. Figure 7 shows the ratio of $\sigma_{gg}^{\text{NNLO}}(M_t^n)$, keeping various orders in $1/M_t$, to the heavy-top result $\sigma_{gg,\infty}^{\text{NNLO}}$ of eq. (3.3), which we recall includes the exact LO mass dependence (dashed: $1/M_t^n$, $n = 0, 2, 4$; solid: $1/M_t^6$). The dotted line corresponds to the pure soft expansion result σ_{gg}^N, without matching to the low-x behaviour. We observe very good convergence towards the heavy-top result, assuring us of the high quality of the latter.

We then apply the same criteria as at NLO in order to obtain the "optimal" result $\sigma^{\text{NNLO}}(M_t)$ for the M_t dependent NNLO terms. They allow us to keep all four available terms for the gg and the qg curve, i.e., through order $1/M_t^6$, and again only the first two terms for the qq, $q\bar{q}$, and qq' initiated sub-processes. The result, divided by the one obtained from eq. (3.3), is shown in figure 8, for various orders in the soft expansion which again converges excellently.

The final result is within 0.5% of the well-known heavy-top limit, clearly justifying its successful and extensive application in the literature. As outlined above, one can now try to improve the NNLO prediction by factoring out the LO top mass dependence. However, it is obvious that this will not alter the result by more than 0.5% which is way below any expected experimental accuracy.

It should be stressed that the accuracy of the heavy-top limit found in our calculation is overshadowed by the current uncertainties arising from the renormalization and factorization scale dependence and parton density functions. Also, interference effects with the bottom induced gluon-Higgs couplings have justifiably been neglected in our study; they may become relevant in supersymmetric models with enhanced bottom Yukawa coupling. In this context, it should also be recalled that NNLO corrections for the bottom induced gluon Higgs coupling are to date unknown; the small bottom quark mass complicates the calculation enormously, and even a feasible approximation scheme has not yet been found.

7 Conclusions and outlook

Top mass effects on the NNLO Higgs cross section in gluon fusion have been calculated. For the dominant gg channel, the result for $\hat{s} < 4M_t^2$ has been matched to the limiting behaviour at $x \to 0$ as obtained in ref. [49]. We have demonstrated the reliability of our result through the excellent convergence of the soft expansion. The main result is the confirmation of the remarkable quality of the heavy-top limit as defined in eq. (3.3) which agrees with the $1/M_t$ expansion to better than 0.5% in the phenomenologically interesting mass range $100\,\text{GeV} \leq M_{\text{H}} \leq 300\,\text{GeV}$, both at the LHC as well as at the Tevatron. This is an extremely comforting result because it validates the numerous higher order analyses

JHEP11(2009)088

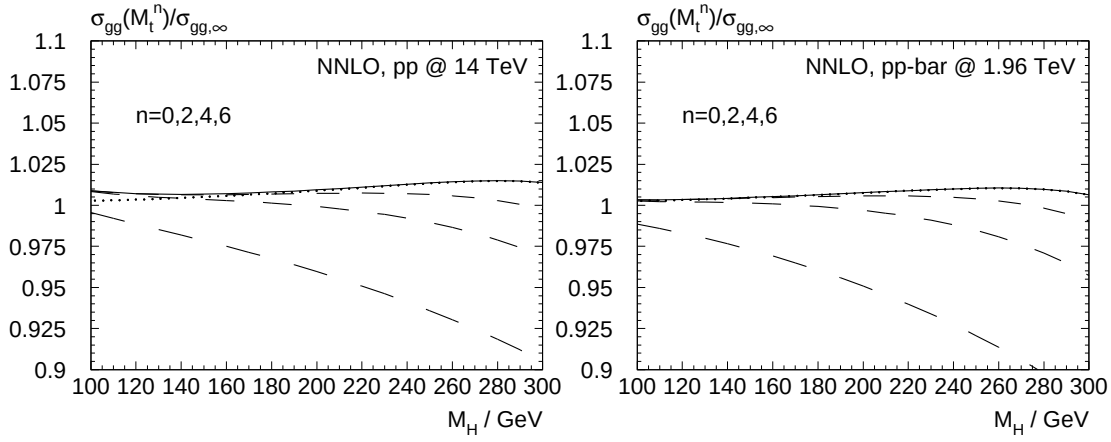

(a) (b)

Figure 7. Ratio of the gg induced component of the NNLO hadronic cross section as obtained from eq. (5.2) to the heavy-top result of eq. (3.3), (decreasing dash-length corresponds to increasing order in $1/M_t$); the dotted line is the result obtained from the pure soft expansion $\hat{\sigma}_{gg}^{(2),N}$ through order $1/{M_t}^6$ without the matching of eq. (5.2).

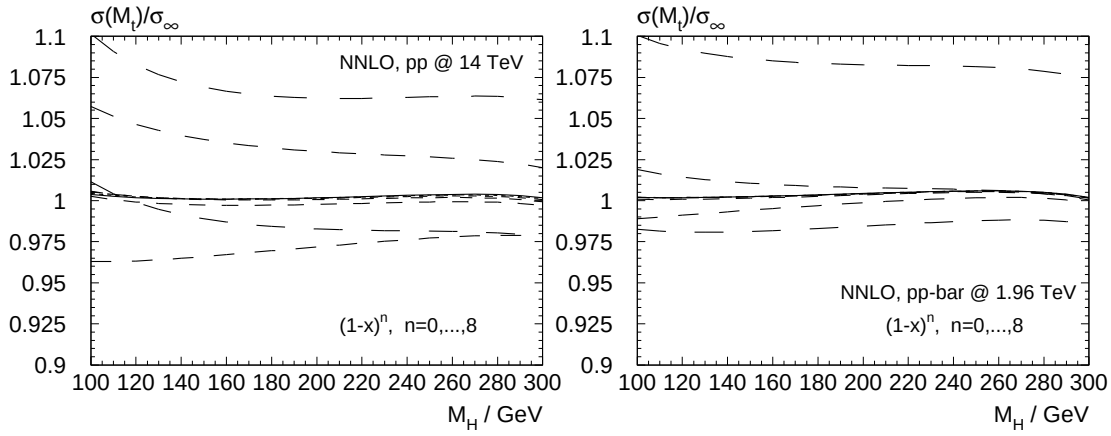

(a) (b)

Figure 8. NNLO version of figure 6, but now the curves are normalized to the heavy-top limit of eq. (3.3).

that have been carried out up to now, in preparation for the LHC experiments [52, 53], and in particular for the ongoing Higgs searches at the Tevatron [54].

It remains to be seen to what extent the findings of our paper carry over to less inclusive quantities like distributions or phase space cuts. This requires a substantial extension of our approach and is left for future studies.

JHEP11(2009)088

Acknowledgments

We would like to thank M. Czakon, V. del Duca, S. Forte, and M. Steinhauser for fruitful discussions. RVH thanks the organizers of the CERN TH institute "SM-BSM physics at the LHC", where part of this work was carried out, for hospitality and financial support. This work was supported by DFG under contract HA 2990/3-1, and the Helmholtz Alliance "Physics at the Terascale".

References

[1] J.F. Gunion, H.E. Haber, G. Kane and S. Dawson, *The Higgs Hunter's Guide*, Addison-Wesley (1990).

[2] A. Djouadi, *The Anatomy of electro-weak symmetry breaking. I: The Higgs boson in the standard model*, *Phys. Rept.* **457** (2008) 1 [hep-ph/0503172] [SPIRES].

[3] A. Djouadi, *The Anatomy of electro-weak symmetry breaking. II. The Higgs bosons in the minimal supersymmetric model*, *Phys. Rept.* **459** (2008) 1 [hep-ph/0503173] [SPIRES].

[4] S. Dawson, *Radiative corrections to Higgs boson production*, *Nucl. Phys.* **B 359** (1991) 283 [SPIRES].

[5] A. Djouadi, M. Spira and P.M. Zerwas, *Production of Higgs bosons in proton colliders: QCD corrections*, *Phys. Lett.* **B 264** (1991) 440 [SPIRES].

[6] D. Graudenz, M. Spira and P.M. Zerwas, *QCD corrections to Higgs boson production at proton proton colliders*, *Phys. Rev. Lett.* **70** (1993) 1372 [SPIRES].

[7] M. Spira, A. Djouadi, D. Graudenz and P.M. Zerwas, *Higgs boson production at the LHC*, *Nucl. Phys.* **B 453** (1995) 17 [hep-ph/9504378] [SPIRES].

[8] R.V. Harlander and W.B. Kilgore, *Next-to-next-to-leading order Higgs production at hadron colliders*, *Phys. Rev. Lett.* **88** (2002) 201801 [hep-ph/0201206] [SPIRES].

[9] C. Anastasiou and K. Melnikov, *Higgs boson production at hadron colliders in NNLO QCD*, *Nucl. Phys.* **B 646** (2002) 220 [hep-ph/0207004] [SPIRES].

[10] V. Ravindran, J. Smith and W.L. van Neerven, *NNLO corrections to the total cross section for Higgs boson production in hadron hadron collisions*, *Nucl. Phys.* **B 665** (2003) 325 [hep-ph/0302135] [SPIRES].

[11] D. de Florian and M. Grazzini, *Higgs production through gluon fusion: updated cross sections at the Tevatron and the LHC*, *Phys. Lett.* **B 674** (2009) 291 [arXiv:0901.2427] [SPIRES].

[12] C. Anastasiou, R. Boughezal and F. Petriello, *Mixed QCD-electroweak corrections to Higgs boson production in gluon fusion*, *JHEP* **04** (2009) 003 [arXiv:0811.3458] [SPIRES].

[13] S. Catani, D. de Florian, M. Grazzini and P. Nason, *Soft-gluon resummation for Higgs boson production at hadron colliders*, *JHEP* **07** (2003) 028 [hep-ph/0306211] [SPIRES].

[14] V. Ahrens, T. Becher, M. Neubert and L.L. Yang, *Origin of the Large Perturbative Corrections to Higgs Production at Hadron Colliders*, *Phys. Rev.* **D 79** (2009) 033013 [arXiv:0808.3008] [SPIRES].

[15] R. Harlander and P. Kant, *Higgs production and decay: Analytic results at next-to-leading order QCD*, *JHEP* **12** (2005) 015 [hep-ph/0509189] [SPIRES].

JHEP11(2009)088

[16] C. Anastasiou, S. Beerli, S. Bucherer, A. Daleo and Z. Kunszt, *Two-loop amplitudes and master integrals for the production of a Higgs boson via a massive quark and a scalar-quark loop*, *JHEP* **01** (2007) 082 [hep-ph/0611236] [SPIRES].

[17] U. Aglietti, R. Bonciani, G. Degrassi and A. Vicini, *Analytic results for virtual QCD corrections to Higgs production and decay*, *JHEP* **01** (2007) 021 [hep-ph/0611266] [SPIRES].

[18] A.D. Martin, W.J. Stirling, R.S. Thorne and G. Watt, *Parton distributions for the LHC*, *Eur. Phys. J.* **C 63** (2009) 189 [arXiv:0901.0002] [SPIRES].

[19] A. Djouadi and P. Gambino, *Leading electroweak correction to Higgs boson production at proton colliders*, *Phys. Rev. Lett.* **73** (1994) 2528 [hep-ph/9406432] [SPIRES].

[20] U. Aglietti, R. Bonciani, G. Degrassi and A. Vicini, *Two-loop light fermion contribution to Higgs production and decays*, *Phys. Lett.* **B 595** (2004) 432 [hep-ph/0404071] [SPIRES].

[21] G. Degrassi and F. Maltoni, *Two-loop electroweak corrections to Higgs production at hadron colliders*, *Phys. Lett.* **B 600** (2004) 255 [hep-ph/0407249] [SPIRES].

[22] S. Actis, G. Passarino, C. Sturm and S. Uccirati, *NLO Electroweak Corrections to Higgs Boson Production at Hadron Colliders*, *Phys. Lett.* **B 670** (2008) 12 [arXiv:0809.1301] [SPIRES].

[23] J.R. Ellis, M.K. Gaillard and D.V. Nanopoulos, *A Phenomenological Profile of the Higgs Boson*, *Nucl. Phys.* **B 106** (1976) 292 [SPIRES].

[24] K.G. Chetyrkin, B.A. Kniehl and M. Steinhauser, *Hadronic Higgs decay to order α_s^4*, *Phys. Rev. Lett.* **79** (1997) 353 [hep-ph/9705240] [SPIRES].

[25] Y. Schröder and M. Steinhauser, *Four-loop decoupling relations for the strong coupling*, *JHEP* **01** (2006) 051 [hep-ph/0512058] [SPIRES].

[26] K.G. Chetyrkin, J.H. Kühn and C. Sturm, *QCD decoupling at four loops*, *Nucl. Phys.* **B 744** (2006) 121 [hep-ph/0512060] [SPIRES].

[27] K.G. Chetyrkin, B.A. Kniehl and M. Steinhauser, *Decoupling relations to $O(\alpha_s^3)$ and their connection to low-energy theorems*, *Nucl. Phys.* **B 510** (1998) 61 [hep-ph/9708255] [SPIRES].

[28] M. Krämer, E. Laenen and M. Spira, *Soft gluon radiation in Higgs boson production at the LHC*, *Nucl. Phys.* **B 511** (1998) 523 [hep-ph/9611272] [SPIRES].

[29] R. Harlander, *Supersymmetric Higgs production at the Large Hadron Collider*, *Eur. Phys. J.* **C 33** (2004) s454 [hep-ph/0311005] [SPIRES].

[30] C. Balázs, M. Grazzini, J. Huston, A. Kulesza and I. Puljak, *A comparison of predictions for SM Higgs boson production at the LHC*, hep-ph/0403052 [SPIRES].

[31] C. Anastasiou, K. Melnikov and F. Petriello, *Higgs boson production at hadron colliders: Differential cross sections through next-to-next-to-leading order*, *Phys. Rev. Lett.* **93** (2004) 262002 [hep-ph/0409088] [SPIRES].

[32] S. Catani and M. Grazzini, *HNNLO: a Monte Carlo program to compute Higgs boson production at hadron colliders*, PoS(RADCOR2007)046 [arXiv:0802.1410] [SPIRES].

[33] W.-Y. Keung and F.J. Petriello, *Electroweak and finite quark-mass effects on the Higgs boson transverse momentum distribution*, *Phys. Rev.* **D 80** (2009) 013007 [arXiv:0905.2775] [SPIRES].

JHEP11(2009)088

[34] C. Anastasiou, S. Bucherer and Z. Kunszt, *HPro: A NLO Monte-Carlo for Higgs production via gluon fusion with finite heavy quark masses*, *JHEP* **10** (2009) 068 [arXiv:0907.2362] [SPIRES];

[35] S. Dawson and R. Kauffman, *QCD corrections to Higgs boson production: nonleading terms in the heavy quark limit*, *Phys. Rev.* **D 49** (1994) 2298 [hep-ph/9310281] [SPIRES].

[36] D. Neill, *Two-Loop Matching onto Dimension Eight Operators in the Higgs-Glue Sector*, arXiv:0908.1573 [SPIRES].

[37] V.A. Smirnov, *Applied asymptotic expansions in momenta and masses*, *Springer Tracts Mod. Phys.* **177** (2002) 1.

[38] R.V. Harlander and K.J. Ozeren, *Top mass effects in Higgs production at next-to-next-to-leading order QCD: virtual corrections*, *Phys. Lett.* **B 679** (2009) 467 [arXiv:0907.2997] [SPIRES].

[39] A. Pak, M. Rogal and M. Steinhauser, *Virtual three-loop corrections to Higgs boson production in gluon fusion for finite top quark mass*, *Phys. Lett.* **B 679** (2009) 473 [arXiv:0907.2998] [SPIRES].

[40] M. Steinhauser, *MATAD: A program package for the computation of massive tadpoles*, *Comput. Phys. Commun.* **134** (2001) 335 [hep-ph/0009029] [SPIRES].

[41] K.G. Chetyrkin and F.V. Tkachov, *Integration by Parts: The Algorithm to Calculate β-functions in 4 Loops*, *Nucl. Phys.* **B 192** (1981) 159 [SPIRES].

[42] T. Seidensticker, *Using* `q2e` *and* `exp`, Universität Karlsruhe, 2002 (unpublished).

[43] R. Harlander, T. Seidensticker and M. Steinhauser, *Complete corrections of $O(\alpha\alpha_s)$ to the decay of the Z boson into bottom quarks*, *Phys. Lett.* **B 426** (1998) 125 [hep-ph/9712228] [SPIRES].

[44] P. Nogueira, *Automatic Feynman graph generation*, *J. Comput. Phys.* **105** (1993) 279.

[45] J. Blümlein and S. Kurth, *Harmonic sums and Mellin transforms up to two-loop order*, *Phys. Rev.* **D 60** (1999) 014018 [hep-ph/9810241] [SPIRES].

[46] R.V. Harlander, *Virtual corrections to $g\ g \to H$ to two loops in the heavy top limit*, *Phys. Lett.* **B 492** (2000) 74 [hep-ph/0007289] [SPIRES].

[47] R.V. Harlander and W.B. Kilgore, *Soft and virtual corrections to $p\ p \to H + X$ at NNLO*, *Phys. Rev.* **D 64** (2001) 013015 [hep-ph/0102241] [SPIRES].

[48] S. Catani, D. de Florian and M. Grazzini, *Higgs production in hadron collisions: Soft and virtual QCD corrections at NNLO*, *JHEP* **05** (2001) 025 [hep-ph/0102227] [SPIRES].

[49] S. Marzani, R.D. Ball, V. Del Duca, S. Forte and A. Vicini, *Higgs production via gluon-gluon fusion with finite top mass beyond next-to-leading order*, *Nucl. Phys.* **B 800** (2008) 127 [arXiv:0801.2544] [SPIRES].

[50] S. Marzani, R.D. Ball, V. Del Duca, S. Forte and A. Vicini, *Finite-top-mass effects in NNLO Higgs production*, *Nucl. Phys. Proc. Suppl.* **186** (2009) 98 [arXiv:0809.4934] [SPIRES].

[51] M. Spira, *HIGLU: A Program for the Calculation of the Total Higgs Production Cross Section at Hadron Colliders via Gluon Fusion including QCD Corrections*, hep-ph/9510347 [SPIRES].

JHEP11(2009)088

[52] CMS collaboration, G.L. Bayatian et al., *CMS technical design report, volume II: Physics performance*, *J. Phys.* **G 34** (2007) 995.

[53] The ATLAS collaboration, G. Aad et al., *Expected Performance of the ATLAS Experiment-Detector, Trigger and Physics*, arXiv:0901.0512 [SPIRES].

[54] CDF collaboration, *Combined CDF and DZero Upper Limits on Standard Model Higgs-Boson Production with up to 4.2 fb^{-1} of Data*, arXiv:0903.4001 [SPIRES].

JHEP11(2009)088